# Influence of Temperature on the Conformation of Canine Plasminogen: An Analytical Ultracentrifugation and Dynamic Light Scattering Study†

Jack A. Kornblatt*,‡ and Peter Schuck§

*Enzyme Research Group, Department of Biology, Concordia University, 7141 Sherbrooke Ouest, Montreal, Quebec, Canada H4B 1R6, and National Institutes of Health, Building 13, Room 3N17, 13 South Drive, Bethesda, Maryland 20892*

*Received May 13, 2005; Revised Manuscript Received August 5, 2005*

ABSTRACT: Plasminogen is known to undergo an extremely large conformational change when it binds ligands; the two well-established conformations are either closed (absence of external ligand) or open (presence of external ligand). We show here that plasminogen is more complicated than can be accommodated by a two-state, closed/open, model. Temperature changes induce large structural changes which can be detected with either dynamic light scattering or analytical ultracentrifugation. The temperature-induced changes are not related to the classical closed/open conformational change since both closed and open forms of the protein are similarly influenced. It appears as though the packing density of the protein increases as the temperature is raised. Over the range 4−20 °C, the Stokes' radius of the classical closed plasminogen goes from 4.7 to 4.2 nm, and that of the classical open form goes from 5.55 to 5.0 nm. These changes in packing can be rationalized if temperature change induces a large conformational change and if this is accompanied by a large change in hydration, by a change in solute binding, or by a change in the total void volume of the protein.

Human plasminogen is a single-chain protein consisting of 791 amino acids organized into an amino-terminal domain, five closely spaced kringle domains, and a proproteolytic domain (for comprehensive reviews see refs *1* and *2*). Canine plasminogen, the protein used throughout this study, consists of 793 amino acids and is about 88% identical to the human form.[1]

Plasminogen is the precursor of the proteolytic enzyme, plasmin. The conversion from the proenzyme to plasmin occurs by cleavage of a single bond between residues 561 and 562 of the 791 residue precursor (*3*). This yields a two-chain enzyme in which the two chains are held together by a disulfide bridge between two cysteine residues. Plasmin has several preferred substrates, the most common of which is fibrin, the major protein of the blood clot. Plasmin is also active on the proteins which hold cells to one another; it thereby facilitates tissue remodeling as well as tumor metastasis. Activation of plasminogen probably requires opening of the protein, but not all ligands that promote opening promote activation. The subject has been well reviewed recently (*4*, *5*).

In 1959 Aikjaersig et al. (*6*) showed that the binding of 6-AH[2] (6-aminohexanoate) to plasminogen induced a large conformational change in the protein. This change has been rigorously characterized by many groups. The protein has been shown to undergo a closed to open transition. The closed form is found in the absence of external ligands. It is maintained by ligation of lysine 50 to a binding site on kringle 5 (*7*−*9*). The open form is induced by ligand binding which displaces the internal ligand. External ligands can be analogues of lysine or amino sugars or water; the latter is a poor ligand.

In an elegant analytical ultracentrifugation study Brockway and Castellino (*10*) determined the influence of 6-aminohexanoate on plasminogen structure and showed that the binding of the ligand lowered the $s_{20,w}$ value of the protein. This was combined with a fluorescence polarization study (*11*) to show that ligand binding induces a large change in polarization indicative of a much more open conformation. The data from the latter study were used to calculate frictional ratios of the closed and open forms. An early electron microscopy study by Tranqui (*12*) showed that a population of plasminogen molecules, in the absence of ligands, actually consisted of a mixture of closed and open forms with the closed predominating. Ligand binding induced the majority of the molecules to open. This study was followed by others that employed neutron scattering (*13*) and small-angle X-ray scattering (*14*). The latter two studies also indicated that the closed to open transition was accompanied by a large change in the Stokes' radius but in quantitative terms they did not give exactly the same results.

† Supported by The Natural Sciences and Engineering Research Council (Canada), Grant 9988-2000, and in part by the Intramural Research Program of the NIH, OD.

* Corresponding author. E-mail: krnblt@vax2.concordia.ca. Tel: 514-848-2424 ext 3404. Fax: 514-848-2881.

‡ Concordia University.

§ National Institutes of Health.

[1] D. Carter, M.Sc. Thesis, Concordia University, 2004.

[2] Abbreviations: AUC, analytical ultracentrifuge; 6-AH, 6-aminohexanoate; DLS, dynamic light scattering; DPGN, canine plasminogen; $\eta$, viscosity at temperature $T$; $f/f_0$, frictional ratio; $KP_i$, potassium phosphate; $k_B$, Boltzmann constant; $M$, molecular weight; $m$, molar mass; $N$, Avogadro's number; $R$, Stokes' radius; $\rho$, density at temperature $T$; $s_T$, sedimentation coefficient at temperature $T$; $s_{20,w}$, sedimentation coefficient corrected to standard conditions in water at 20 °C; $\bar{v}_2$, partial specific volume of the protein at temperature $T$.

10.1021/bi050895y CCC: $30.25 
Published on Web 09/10/2005

We have used, in this study of temperature effects on plasminogen, the analytical ultracentrifuge and dynamic light scattering. Both ultracentrifugation and dynamic light scattering analysis have been applied to plasminogen before (vida supra). The data that were taken, in previous studies, were of very high quality and provided definitive answers regarding the classical closed and classical open forms of the protein. Why bother repeating experiments that, in the past, were done so well? The answer is that the apparatus has improved immensely, and data analysis has improved even more. In the past, it was extremely difficult to determine $f/f_0$ and $s_{20,w}$ in a single experiment; it is now far easier. What kind of information can we get out of a combined DLS, AUC analysis? We can determine whether the apparent buoyant molecular mass of plasminogen is constant over a given temperature range. If it is not, it indicates that the molecule changes either its hydration shell, changes the extent to which it binds solutes, or changes the total excluded volume as one shifts from one temperature to another. Any of the three possibilities would result in a change in $\bar{v}_2$, the effective partial specific volume of the protein.

We report here that the classical closed form of plasminogen responds to increases in temperature by assuming a tighter conformation. The classical open form shows similar behavior, which indicates that the transition is the result of a general repacking of the plasminogen molecule.

## MATERIALS AND METHODS

*Protein Purification.* The preparation of DPGN (canine plasminogen) has been described (*15*); it was stored under vacuum in flame-sealed vials. Aprotinin (0.3 $\mu$M) (Sigma Chemical Co., Oakville, Ontario, Canada) was included in all purification steps. Before use, vials were opened, brought back to their original volume, and dialyzed (3×) to equilibrium against a buffer containing 5 mM dipotassium hydrogen phosphate, 5 mM monopotassium dihydrogen phosphate, and 100 mM sodium chloride. The pH of this solution is about 6.5 and is relatively stable over the 35 °C temperature range used in this study. The experiments with the closed form of DPGN used this buffer directly. The experiments with the open form of DPGN also contained 20 mM 6-AH. The integrity of the DPGN was verified by SDS−PAGE before it was freeze-dried, after the sample was dialyzed, and after an ultracentrifuge run. If there were any indications of conversion to Lys-plasminogen (proteolytic cleavage of the protein between residues 77 and 78) or to plasmin (proteolytic cleavage between residues 561 and 562), the sample and data were discarded (*16*). The protein, after denaturation, is a single species as judged by SDS−PAGE. The native DPGN, in the AUC, sedimented as a single symmetrical species (see below).

*Dynamic Light Scattering.* Dynamic light scattering was measured on a Protein Solutions DynaPro 99 with a DynaPro-MSTC200 microsampler (Protein Solutions, Charlottesville, VA) apparatus with temperature control maintained by a Peltier junction. The scattering signal was observed at an angle of 90°, at a wavelength of 808.3 nm. Temperature fluctuations were approximately ±0.1 °C during the course of a measurement. A sufficient number of counts was collected such that the root mean square deviation (RMSD), the difference between the fitted line and the actual data points, was less than 0.1%. The DLS data were analyzed using Sedfit 8.8 (available at www.analyticalultracentrifugation.com).

*Analytical Ultracentrifugation.* The analytical ultracentrifuge used was an Optima XL-I (Beckman Coulter Instruments, Fullerton, CA) running between 2 and 37 °C. The temperature limitations are set by the centrifuge. Above 37 °C, our machine spits oil into the rotor chamber. The runs were performed over a range of velocities depending on the temperature. The maximum velocity at 4 °C was 40000 rpm; the minimum velocity was 21000 rpm at 33 °C. The data were all taken using absorption optics with a wavelength of 280 nm. The protein concentration was kept at 5 $\mu$M, giving an $A_{280}$ of 0.65. Data analysis was performed using the program Sedfit 8.0 (available at www.analyticalultracentrifugation.com), using the model of a $c(s)$ distribution of Lamm equation solutions (*17*−*20*). Molecular weight distributions on five samples covering the range 4−30 °C were calculated using the values determined from the $c(s)$ distributions and the calculated $\bar{v}_2$ values. The actual molecular weight of DPGN is 88964 without its carbohydrate and 90109 as determined by MALDI-MS on the carbohydrate-containing protein used in this study (J. A. Kornblatt, unpublished results). The five values obtained from the analysis of the sedimentation velocity data yielded a MW of 92107 ± 1145 (SD), indicating that there were no *large* errors in our analysis.

To study the possible effects on the sedimentation profiles from a kinetically controlled conformational change, a Lamm equation model describing the sedimentation of such a system was implemented as an extension of the software SEDPHAT (www.analyticalultracentrifugation.com) using numerical methods outlined in Dam et al. (*21*).

*Hydrodynamic Analysis.* The behavior of any molecular species in the ultracentrifuge is governed by the Svedberg equation:

$$s = \frac{M(1 - \bar{v}_2\rho)}{Nf} \tag{1}$$

where $s$ (in svedbergs) is the sedimentation coefficient; the product $M(1 - \bar{v}_2\rho)$ is the buoyant molecular weight of the sedimenting particle and $\bar{v}_2$ its apparent partial specific volume; $\rho$ is the density of the solution, $N$ is Avogadro's number, and $f$ is the translational frictional coefficient (*22*). A condition for the validity of eq 1 is that *the translational frictional coefficient for sedimentation is the same as the frictional coefficient for translational diffusion*; i.e., the molecule does not deform in the hydrodynamic drag during sedimentation. The assumption seems reasonable since sedimentation is done under conditions where the migration from sedimentation is comparable in order of magnitude to $(D_T t)^{1/2}$.

At any given temperature, buffer density, and viscosity, the sedimentation coefficient can be corrected to standard conditions:

$$s_{20,w} = s_{T,buffer}\frac{(1 - \bar{v}_2\rho)_{20,w}}{(1 - \bar{v}_2\rho)_{T,buffer}}\frac{\eta_{T,buffer}}{\eta_{20,w}} \tag{2}$$

This correction to standard conditions requires precise estimations of the apparent partial specific volume ($\bar{v}_2$) of

the protein at the temperature used, the buffer density at the temperature used, and the viscosity at the temperature used. Since

$$s_{20,w}f_{20,w} = m(1 - \bar{v}_2\rho)_{20,w} \quad (3)$$

it follows that under standard conditions both sides can be divided by the frictional coefficient of an equivalent *unhydrated* sphere under standard conditions, $f_{0,20,w}$.

$$s_{20,w}(f/f_0)_{20,w} = \frac{m(1 - \bar{v}_2\rho)_{20,w}}{f_{0,20,w}} \quad (4)$$

The importance of this equation is that it indicates that the product $s_{20,w}(f/f_0)_{20,w}$ should be independent of the temperature at which the initial measurement was made, as long as the mass of the particle, its associated hydration shells, and its partial specific volume remain constant. [The expression equation (eq 4) is equivalent to the well-known relationship of the temperature-corrected ratio $s_{20,w}/D_{20,w}$ and the buoyant molecular mass at standard conditions.]

The apparent partial specific volume contains contributions from the densely packed, covalently attached atoms, as well as the void spaces between the covalently attached atoms, noncovalently bound solutes, and water. The values for $\bar{v}_2$ at different temperatures were calculated from the DPGN amino acid sequence, neglecting the small contributions from the carbohydrate component. For this, we used the program SEDNTERP which was authored by D. B. Hayes, T. Laue, and J. Philo; the program is available at http://www.jphilo-.mailway.com/ and is kindly provided by Dr. J. Philo. The principles and tabulated data for calculating $\bar{v}_2$ values in SEDNTERP can be found in Laue et al., Perkins, and Cohn (*23*−*25*). The Laue et al. program lists all of the equations necessary including the temperature corrections based on the data in Durchschlag (*26*).

In contrast to ultracentrifugation, the analysis of DLS data is insensitive to partial specific volume and solvent density but is dependent on viscosity. The diffusion coefficient ($D_T$), the Stokes' radius ($R$), or the translational friction coefficient ($f_T$) can be obtained in a DLS experiment. They are related since

$$D_T = \frac{k_B T}{6\pi\eta R} = \frac{k_B T}{f_T} \quad (5)$$

and

$$f_T = 6\pi\eta R \quad (6)$$

where the subscript $T$ denotes the temperature dependence of the quantities at the experimental condition arising from the temperature dependence of the solvent. In terms of our analysis

$$s_T = \frac{m(1 - \bar{v}_2\rho)}{6\pi\eta R} \quad (7)$$

or

$$m = s_T R \frac{6\pi\eta}{1 - \bar{v}_2\rho} \quad (8)$$

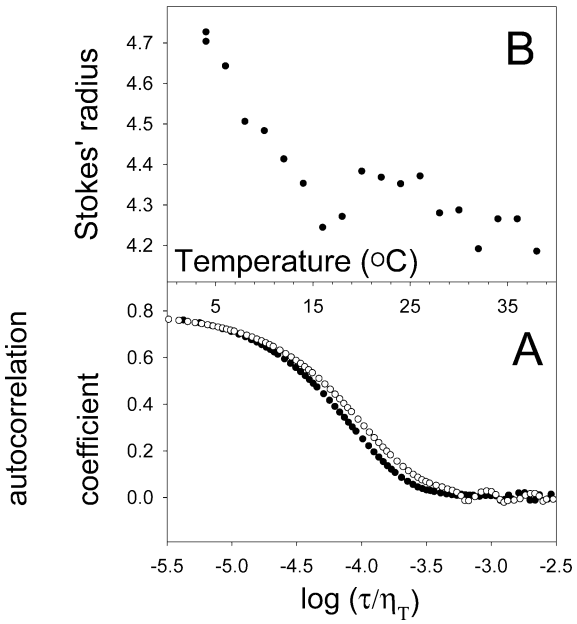


FIGURE 1: Dynamic light scattering of closed DPGN as a function of temperature. The protein concentration was 5 $\mu$M; the buffer was 10 mM $KP_i$ and 100 mM NaCl, pH 6.5. The two curves in (A) are data for two temperatures: 6 °C (open circles) and 38 °C (closed circles). In this plot, the correlation times of the experimental data are scaled with the relative viscosity of the buffer; this eliminates differences of the autocorrelation data stemming from buffer viscosity. The calculated Stokes' radii as functions of temperature are presented in (B).

Once again, after correction for the buffer-related temperature dependence, the equation indicates that the product, $s_T R$, should be independent of temperature provided the buoyant molar mass of the particle, plasminogen in this case, is constant.

The temperature dependence of the properties of DPGN led us to consider two forms, referred to as $DPGN^{LT}$ and $DPGN^{HT}$:

$$DPGN^{LT} \leftrightarrow DPGN^{HT} \qquad K_{eq} = \frac{DPGN^{HT}}{DPGN^{LT}} \quad (9)$$

Since the sum $DPGN^{LT} + DPGN^{HT}$ is constant in any single experiment, the equilibrium populations of both species were modeled as *a sigmoid function in which the position of the equilibrium is related to* $s_T 6\pi\eta/(1 - \bar{v}_2\rho)$ *or* $R$. This is clearly acceptable for the Stokes' radius and is acceptable for $s_T 6\pi\eta/(1 - \bar{v}_2\rho)$ provided the range is small.

## RESULTS

We have used dynamic light scattering to obtain a measure of the influence of temperature on the diffusion characteristics of the closed and open forms of DPGN. The data are presented in Figures 1 and 2. The raw data for both forms at two temperatures are presented in panels A, which show the distribution of autocorrelation coefficients as functions of the decay time, scaled with the relative viscosity for better comparison at the two temperatures. The two curves in each panel do not appear to be very different, but it must be kept in mind that the abscissa extends over 3 log units. The data, at any single temperature, were consistent with a single species (or two rapidly equilibrating species) giving rise to the scattering; the RMSD were less than 0.1%. The signifi-

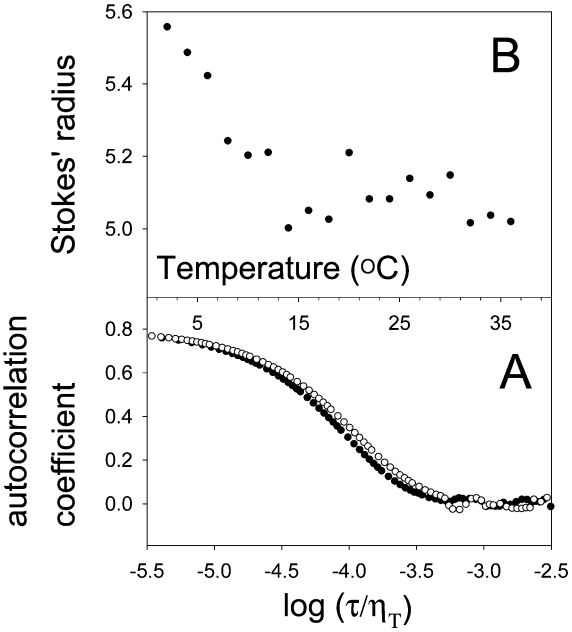


FIGURE 2: Dynamic light scattering of open DPGN as a function of temperature. The protein concentration was 5 $\mu$M; the buffer was 10 mM $KP_i$ and 100 mM NaCl, pH 6.5. The two curves in (A) are data for two temperatures: 2 °C (open circles) and 36 °C (closed circles). In this plot, the correlation times of the experimental data are scaled with the relative viscosity of the buffer; this eliminates differences of the autocorrelation data stemming from buffer viscosity. The calculated Stokes' radii as functions of temperature are presented in (B).

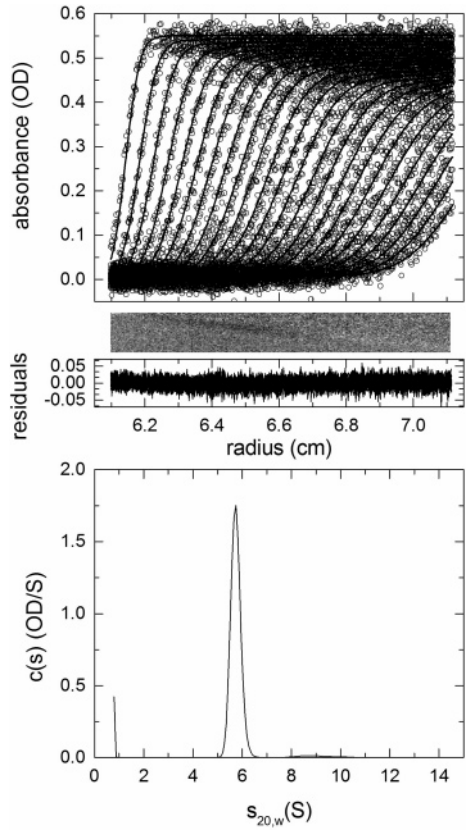


FIGURE 3: Analytical ultracentrifugation of closed DPGN at 4 °C. The protein concentration was 5 $\mu$M; the buffer was 10 mM $KP_i$ and 100 mM NaCl, pH 6.5. Sedimentation was carried out at 42000 rpm. Top panel: Raw sedimentation data (circles, every fourth scan shown) and fit with the *c*(*s*) model (solid lines). The middle panels show the residuals of the fit, in bitmap (*43*) and overlay representation, respectively. The best-fit *c*(*s*) distribution, with $f/f_0$ of 1.35, is shown in the bottom panel. The small peak at 9 S from aggregates amounts to 2.3% of the material.

cant features, of the curves in the two panels A, are that the data for the higher temperature curves are displaced toward smaller correlation times; i.e., the higher the temperature, the smaller the Stokes' radius. The significant information is presented in panels B, which show that the Stokes' radii of the two forms are not constant as temperature is varied. Both closed and open forms become tighter as temperature is raised; the Stokes' radii decrease by about 10% in both cases as *T* goes from the lower values to the higher. The two DLS data sets do not overlap, indicating that, over this range, temperature changes do not force the opening of the closed form nor the closing of the open. As expected, the Stokes' radii for the open form are larger than those for the closed form, but the radii of the closed form decrease further at higher temperature. The results presented in Figures 1A and 2A are quantitatively similar to results obtained in the past (*8*) at a single unspecified temperature.

Next, we studied the temperature-dependent behavior of DPGN in the AUC. Figure 3 shows an example of the sedimentation analysis for closed DPGN at 4 °C. The *c*(*s*) distribution fits the data very well and exhibits a single major peak, indicating a high degree of purity of the material. The analysis could resolve a 9S aggregate, amounting to 2.3% of the loaded material, which was excluded from consideration in determining $s_{20,w}$. A fit with a single-species Lamm equation solution resulted in a fit with an RMS error of 0.0157 OD, slightly worse than that of the *c*(*s*) model (0.0153 OD), and an apparent molar mass of 74.9 kDa. The increased error as well as the significantly smaller molar mass can be attributed to the trace impurities (unresolved in this model) or possible microheterogeneity in DPGN causing the boundary broadening to be slightly inconsistent with a single-species diffusion. This finding is in line with the well-known exquisite sensitivity of the single-species sedimentation model [see Dam et al. (*21*, *27*)]. In contrast, the description of boundary spreading via the $f/f_0$ parameter from the *c*(*s*) analysis is affected by heterogeneity to a much lesser extent (or not at all if the trace species have equal $f/f_0$). This is illustrated by the fact that the combination of $f/f_0$ and *c*(*s*) yields molar mass distributions *c*(M) which peak at 92.1 ± 1.1 kDa (data not shown); this is consistent with the molar mass of 90.1 kDa determined by MALDI-MS and is within the common residual uncertainty resulting from the apparent partial specific volume. Thus, the further analysis of the velocity and spreading of the sedimentation boundary was carried out considering $s_{20,w}$ from the *c*(*s*) peak and the weight-average $f/f_0$, as outlined in eq 4.

We have titrated DPGN at constant temperature with increasing concentrations of 6-AH to observe the change from the closed to the open DPGN conformation (Figure 4). The large change in $s_{20,w}$ has been reported before (*10*). Applying eq 4, we found that the product of $s_{20,w}$ and $f/f_0$ remains essentially constant, indicating that the buoyant molar mass of DPGN does not significantly change from the open to closed transition.

For the study of the temperature-dependent behavior of the open and closed state, we have used DPGN in the presence and absence of 20 mM 6-AH. We were concerned

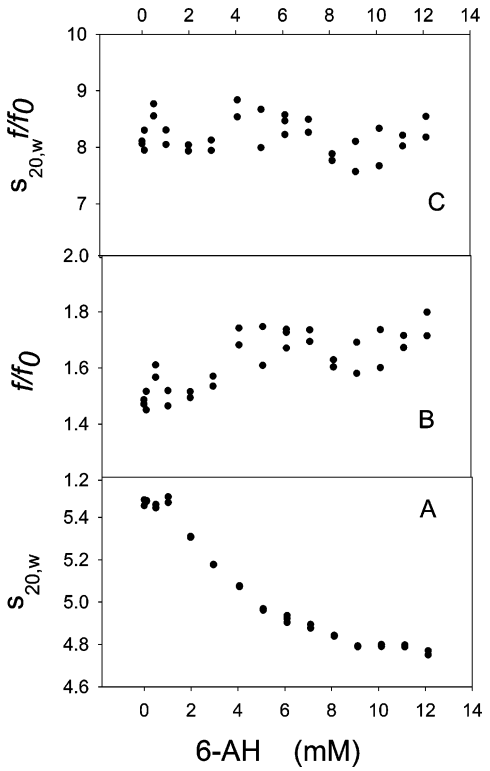


FIGURE 4: Analytical ultracentrifugation of DPGN as a function of the closed to open transition. The protein concentration was 5 $\mu$M; the buffer was 10 mM $KP_i$ and 100 mM NaCl, pH 6.5. The data were collected at 15 °C. Successive amounts of 6-AH were added to the solution being centrifuged. (A) $s_{20,w}$ as a function of 6-AH. (B) The frictional ratio as a function of [6-AH]. (C) The product $s_{20,w}(f/f_0)$ as a function of [6-AH]. The data of (C) indicate that the product term is constant as it should be provided there is no change in buoyant molar mass of the sedimenting particle.

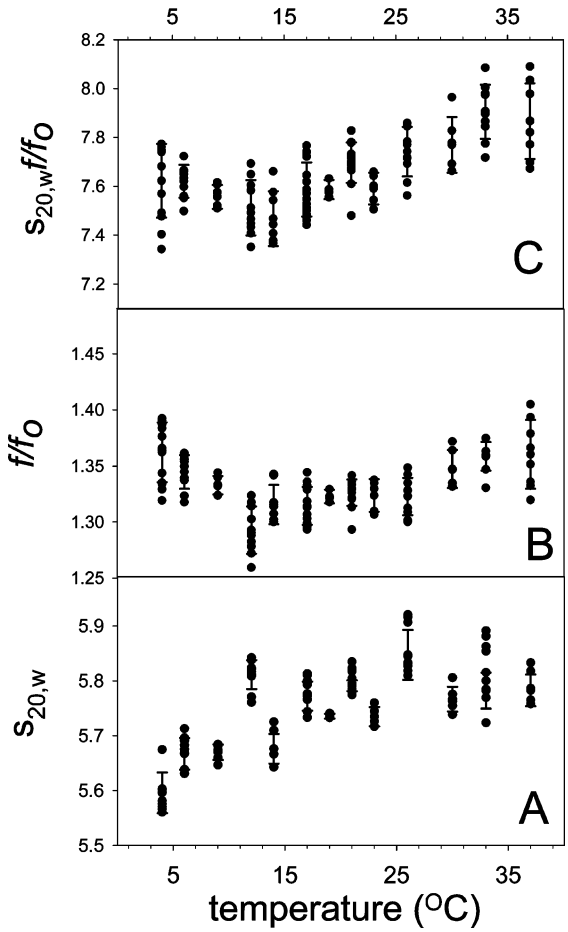


FIGURE 5: Analytical ultracentrifugation of DPGN as a function of temperature: closed DPGN. The protein concentration was 5 $\mu$M; the buffer was 10 mM $KP_i$ and 100 mM NaCl, pH 6.5. Three samples minimum were run at each temperature; each sample was subjected to at least two separate fitting routines in Sedfit. The values of $s$ and $f/f_0$ were obtained from the fitting routine and were chosen on the basis of yielding the best RMSD value. (A) $s_{20,w}$ as a function of temperature. (B) The frictional ratio as a function of temperature. (C) The product $s_{20,w}(f/f_0)$ as a function of temperature.

that under our conditions DPGN may not exist as pure conformational states but exhibit interconverting mixtures of predominantly open molecules with residual fractions of closed molecules, and vice versa. How does the interconversion of conformers influence the evaluation of the product $s_{20,w}(f/f_0)$, a measure of the buoyant molar mass? We carried out computer simulations for the sedimentation boundaries of DPGN assuming a conformational equilibrium relaxing on different time scales. Our centrifugal parameters, concentrations, and signal/noise parameters were those of the experiment shown in Figure 3. We calculated theoretical sedimentation profiles of a mixture of 80% closed and 20% open molecules, interconverting with rate constants of $10^{-6}$/s, $3 \times 10^{-4}$/s, and 0.1/s (data not shown).

When we analyzed these simulated data with a single-species Lamm equation model fitting $s$ and an apparent diffusion coefficient, we obtained the correct weight-average sedimentation coefficient in all cases, but the correct apparent diffusion coefficient only for the rapidly interconverting case. The slowly interconverting mixture resulted in a 10% overestimate of the apparent diffusion coefficient and 4% overestimate when the interconversion was on the time scale of sedimentation ($3 \times 10^{-4}$/s). These results can be expected, due to the excess boundary spread caused by heterogeneity. In contrast, in the $c(s)$ analysis both the fast and the slow interconversion data resulted in the correct weight-average $f/f_0$ value [with the slow case exhibiting a slightly broadened $c(s)$ peak]; only the intermediate case produced an $f/f_0$ value underestimated by 2%. This can be attributed to the ability of the $c(s)$ distribution to account for heterogeneity and to partially compensate for chemical reactions in the form of species with intermediate $s$-values; Dam and Schuck (*28*) discuss this in the context of Gilbert−Jenkins theory. Our analysis indicates that the $c(s)$ approach shows a high degree of robustness against impurities when there are interconverting conformers.

If our samples were highly impure and if the interconversion of conformers were slow on the time scale of sedimentation, our assessment of $f/f_0$ would be in error even while maintaining the correct $s_{20,w}$ value; in such a case, the product, $s_{20,w}(f/f_0)$, would also be in error. This is not the case here; the DPGN is highly pure, and the rate constant of the conformational transition is greater than 10/s (*29*). Therefore, both $s_{20,w}$ and $f/f_0$ reflect weight-average quantities, which, for the DPGN/temperature case, support the use of the product $s_{20,w}(f/f_0)$ as a faithful measure for changes in the buoyant molar mass.

The influences of temperature on the behavior of "closed" DPGN in the AUC are dependent on the temperature range (Figure 5A). Between approximately 15 and 37 °C temperature has little influence on $s_{20,w}$. Between 4 and 15 °C

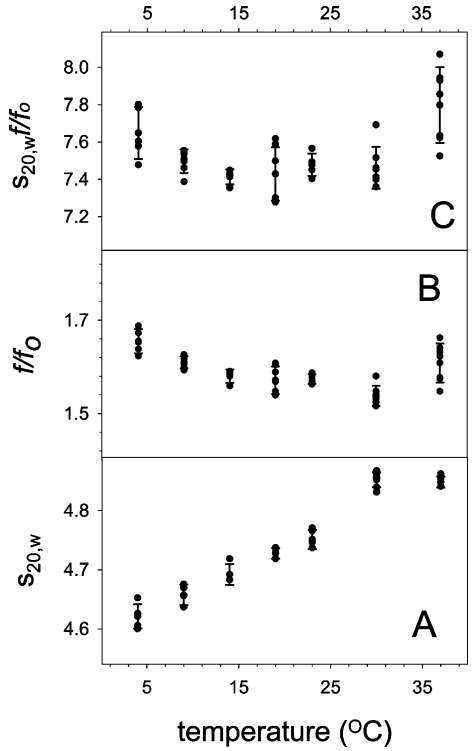


FIGURE 6: Analytical ultracentrifugation of DPGN as a function of temperature: open DPGN. The protein concentration was 5 $\mu$M; the buffer was 10 mM $KP_i$, 100 mM NaCl, and 20 mM 6-AH, pH 6.5. Duplicate samples were run at each temperature. Each was subjected to at least two separate fitting routines. (A) $s_{20,w}$ as a function of temperature. (B) The frictional ratio as a function of temperature. (C) The product $s_{20,w}(f/f_0)$ as a function of temperature.

temperature causes $s_{20,w}$ for the classical closed form to increase by 3%. The changes occurring in the "open" form (Figure 6A) are similar to those occurring with the closed form. $s_{20,w}$ increases as a function of temperature but does not plateau until 30 °C; the total increase in $s_{20,w}$ is about 5%.

The frictional ratios, $f/f_0$, for both the closed and open forms go through minima (Figures 5B and 6B). For the closed form this minimum occurs at 20 °C while it occurs at about 30 °C for the open form. It is important to emphasize that the information content of $f/f_0$ arises from different features of the sedimentation data than the *s*-value (displacement versus spreading of the boundary).

The product terms $[s_{20,w}(f/f_0)]$, which should be constant for both the closed and open forms if the plasminogen buoyant molecular mass is constant, go through minima as seen in Figures 5C and 6C. Even though the products are not constant as a function of temperature, the products exhibit roughly the same temperature dependence for the closed and open form as seen in Figure 7. This suggests that whatever temperature changes are doing to the closed form, they are also doing to the open form.

Both the DLS data and the AUC data indicate that there are at least two conformations of the closed form of DPGN and two of the open form. The simplest assumption is that there are two conformations of each and that there are no measurable intermediates in the conversion between the two. If the deviations from constant product shown in Figures 5 and 6 (panels C) are the result of poor estimation of $f/f_0$, it should be possible to determine this by examining the product

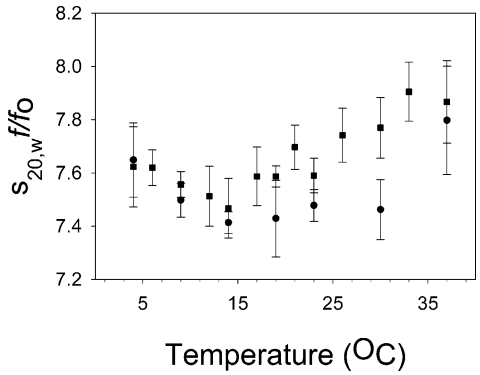


FIGURE 7: Comparison of the variation of the product terms, $s_{20,w}$-$(f/f_0)$, for the closed and open forms of DPGN as functions of temperature. Key: solid squares, closed DPGN; solid circles, open DPGN.

of $s_T 6\pi\eta/(1 - \bar{v}_2\rho)$ and the Stokes' radius *R* (eq 8). This combines the more accurate features of both AUC and DLS. The two experiments were not run at the same temperatures. To multiply them together, both *R* and $s_T 6\pi\eta/(1 - \bar{v}_2\rho)$ were modeled as sigmoid functions of temperature as described in Materials and Methods. The modeled data, shown as the solid lines, for the closed and open forms are presented in Figures 8 and 9. Panels A show the fits (solid line) for the AUC data and panels B the comparable fits (solid line) for the DLS data. Panels C show the product obtained by multiplying the solid line from the AUC fit with that from the DLS fit, a presentation that highlights the trends of the combined temperature dependence. There is only one important point: the product terms, $s_T R 6\pi\eta/(1 - \bar{v}_2\rho)$, are not constant as they would be for a constant buoyant molar mass. For both the closed and open forms, the products go through a minimum and appear to plateau at the higher temperatures. The origin of the minimum is the difference in the midpoint of the temperature dependence in the AUC and DLS data.

We have repeatedly alluded to the fact that there is a major conformational change associated with the opening and closing of DPGN. This is not an original claim. The classical plasminogen conformational change was, for a long time, the second largest known. From the point of view of this study, $s_{20,w}$ changes; the frictional ratio changes and the Stokes' radius changes as the protein undergoes an open/closed transition. Clearly, an equilibrium between the two conformations exists, and residual conformational "impurities" are present under the experimental conditions designed to observe the "closed" and "open" states. Is the open/closed transition responsible for the large change in $s_{20,w}$ , frictional ratio, and Stokes' radius that we see as a function of temperature? The answer can only be "no".

1. In the AUC experiments at different temperatures, all of the changes seen in the closed form are also seen in the open form. The product, $s_{20,w}(f/f_0)$, is about the same in both cases as can be seen in Figure 7. This argues that the product $s_{20,w}(f/f_0)$ is independent of the well-studied classical conformations. The same argument applies to the DLS data.

2. The changes in $s_{20,w}(f/f_0)$ for both classical forms reach a minimum at about 20 °C. The changes in Stokes' radius reach a plateau at about 20 °C. Both types of experiment indicate that a final form has been attained at the elevated temperatures.

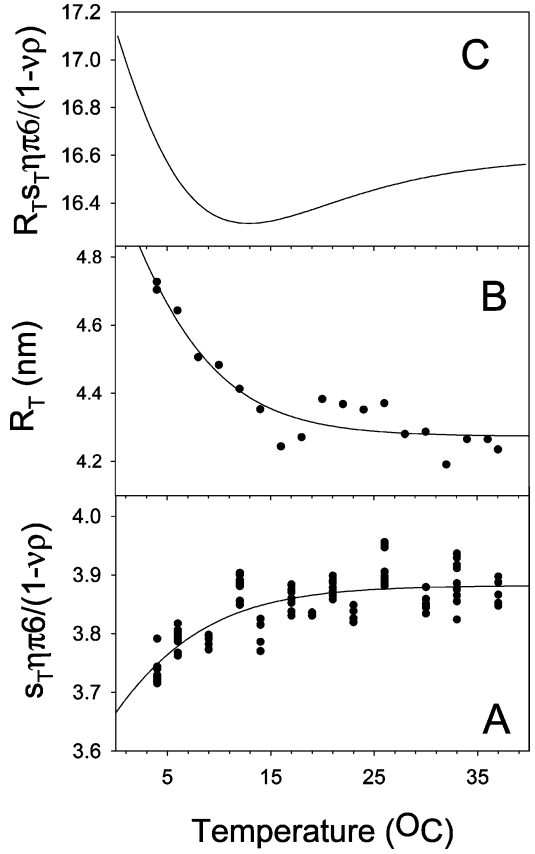


FIGURE 8: The combined dynamic light scattering and analytical ultracentrifugation data also vary as functions of temperature. DPGN, the closed form. (A) A sigmoid curve was fit to the corrected *s*-value as a function of temperature to simulate the behavior of eq 9. The conditions are from Figure 5. (B) The Stokes' radius as a function of temperature (from Figure 1). A sigmoid curve was fit to the data. (C) The product terms: the sigmoid curve of (A) times the sigmoid curve of (B). This treatment was necessary for a comparison of the two data sets since they were not performed at the same temperature.

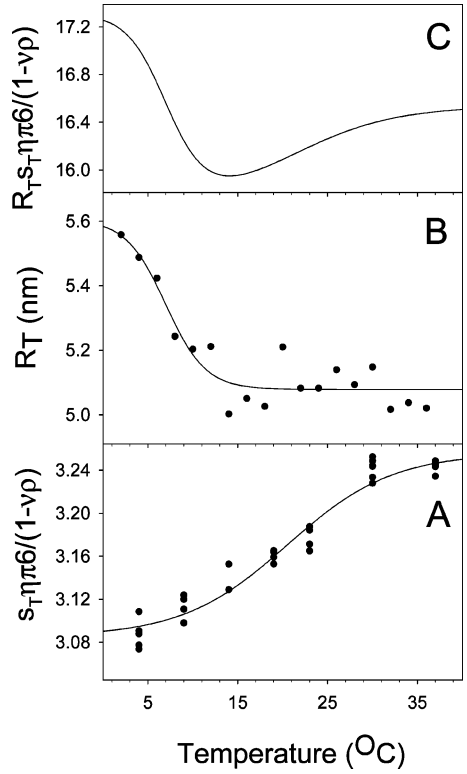


FIGURE 9: The combined dynamic light scattering and analytical ultracentrifugation data also vary as functions of temperature. DPGN, the open form. (A) A sigmoid curve was fit to the corrected *s*-value as a function of temperature to simulate the behavior of eq 9. The conditions are from Figure 6. (B) The Stokes' radius as a function of temperature (from Figure 2). A sigmoid curve was fit to the data. (C) The product terms: the sigmoid curve of (A) times the sigmoid curve of (B). This treatment was necessary for a comparison of the two data sets since they were not performed at the same temperature.

3. A titration of the closed form to the open has been carried out. This was an AUC study. The data are presented in Figure 4. The $s_{20,w}$ decreases as the protein opens as has been seen in many studies. The frictional ratio increases as the protein opens. The product $s_{20,w}(f/f_0)$ remains more or less constant. The aberrant behavior seen in the top panels of Figures 5 and 6 and mimicked in the two DLS figures is the result of more than just the protein opening or closing.

## DISCUSSION

Regarding the data that have been presented here, there are two linked questions that must be answered. Question 1: Are the data reasonable or are they the result of some systematic artifact? Question 2: If the data are not the result of systematic artifacts, what do they mean in terms of plasminogen structure?

1. Reasonable or artifact? We have used two independent techniques that rely on different assumptions. The only dependencies they have in common are size/shape and viscosity. The accuracy with which $s_{20,w}$ (AUC) and the Stokes' radius (DLS) are determined is high whereas the accuracy of determining $f/f_0$ is lower.

The temperature-induced changes in plasminogen are not the result of aggregation; the molecular weights that we calculate from the AUC data differ from the MALDI-MS molecular mass by less than 2.5%, which is within the usual error of the absolute values of molecular mass arising mostly from uncertainties in the estimation of the partial specific volume. We have used an approach for sedimentation analysis that allowed us to resolve and quantify a low level of stable aggregates and prevent it from producing bias in the estimate of the buoyant molar mass. Although not as stringent as in AUC, the autocorrelation data from DLS also allowed us to monitor the size distribution of the protein and rule out significant aggregation. Low levels of rapidly reversible oligomerization would have been resolved in neither the *c*(*s*) analysis of the AUC data nor the DLS data. In theory, it would be consistent with a systematic increase of $s_{20,w}$ with temperature but would also result in an increase of the Stokes' radius with increasing temperature, which is opposite of what we have measured.

If there were signs of aggregation in our samples as temperature was lowered, we could ascribe the radius changes to cold-induced denaturation. In addition to analytical ultracentrifugation and dynamic light scattering, we have used UV derivative spectroscopy, circular dichroism (240−320 nm), fluorescence, and fluorescence anisotropy in order to see if any of the four techniques would report on the changes seen in AUC and DLS. Not one of the four other techniques was sufficiently sensitive such that it could detect temperature-induced changes. These negative results are

important; they indicate that the changes we have seen are not transmitted to the inner portions of the six tightly folded domains. We are probably not dealing with an equilibrium between a native state and a molten globule or denatured state. There are no indications that aggregation is occurring. Viscosity of the solvent system is the solvent parameter that links the two types of measurements. Have the viscosities, which are ultimately those published in the *Handbook of Chemistry and Physics*, been accurately determined? Viscosities of a weakly buffered sodium chloride solution are, for the most part, the result of the characteristics of water. The most accurate data are based on the values given by Swindells, Coe, Jr., and Godfrey (*30*) and were the viscosities used for the AUC and DLS determinations reported here. If they are in error, the errors are common to all viscosity-based data taken over the last 50 years.

We feel that the frictional ratio data, the $s_{20,w}$ data, and their products indicate that there are at least two different conformations accessible to plasminogen in addition to the two classical conformations. Similarly, we feel that the dynamic light scattering data indicate at least two conformations that differ from the classical conformations and that at low temperature these have Stokes' radii greater than the classical forms. Most importantly, either the new conformations differ from the classical forms by a very large degree or there is a serious error in the use of the two techniques applied here. We clearly believe that DPGN undergoes a very large thermally induced transition. The data, as far as we can determine, are not the result of systematic artifacts.

2. What do the data mean in terms of structure? Plasminogen is not like other proteins. It consists of a flexible N-terminal domain and six tightly packed domains connected by short spacers. Kringles 2 and 3 are also liked by a disulfide bridge (*31*). The entire protein is tied together by a weak bond between the first and sixth domain, the N-terminal peptide, and kringle 5. We have described the overall molecule as a necklace containing five beads (kringles 1−4, the proteolytic domain) in which the hasp, the noncovalent bond between Lys50 and kringle 5, is relatively weak (*32*). The terminology is not important. What is important is to recognize that DPGN is a flexible molecule and that it can open and close. The kringles and the proteolytic domain must be in very close proximity to one another and must be capable of readjusting their positions relative to one another; the overall molecule can contract (high temperature) or expand (low temperature). Electron micrographs of the closed plasminogen show what appear to be well-packed doughnuts with the kringle domains protruding out from the central cavity (*33*). The thickness of the doughnuts is consistent with the kringles protruding obliquely from the plane of the doughnut. Chemical cross-linking experiments have shown that kringle 2 is close to the catalytic domain of plasminogen (*34*).

We propose that as the temperature is lowered below 15 °C, the kringles and the proteolytic domains move more into the plane of the doughnut, thereby increasing the Stokes' radius. As the kringles move out, away from the tight packing of the high-temperature form, the entire molecule either becomes more hydrated, changes its bound solute content, or opens (or expands) new voids; any or all of the three would result in changes in the partial specific volume.

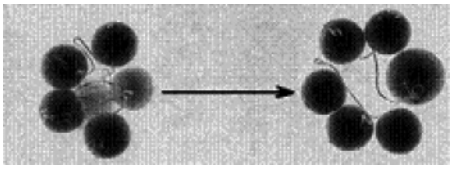

FIGURE 10: Styrofoam ball model of plasminogen. The kringles, proteolytic domain, and linkers have all been scaled relative to one another. The high-temperature compact form is on the left. Kringle 5 is slightly out of the plane of the other kringles, and the catalytic domain is totally out of the plane but close to kringle 2. Tilting the compact form shows a clear doughnut hole through the molecule. By rotating kringle 5 and the catalytic domain into the plane formed by kringles 1−4, the entire molecule becomes planar and the close contact between kringle 2 and the catalytic domain is abolished.

The partial specific volume of a large number of proteins has been determined as a function of temperature; temperature vs partial specific volume is linear over the range 4−45 °C. The data have been summarized and reviewed by Durchschlag (*26*) and implemented in the software SEDNTERP. On average, proteins undergo thermal expansion (the partial specific volume increases) at higher temperature. Unfortunately, the precision of the temperature dependence of the partial specific volume of "average" proteins may be limited, and the empirical nature of the tabulated values makes it likely that they compound several contributing factors. Durchschlag (*26*) points out that peptides and denatured proteins exhibit a stronger temperature dependence vis-à-vis native proteins, suggesting that hydration plays a significant role in the thermal expansion. But for the interpretation of our current data, it seems operationally useful to consider the temperature-dependent changes beyond the average expected density changes for polypeptide chains. On the basis of average values, we would predict a 3% decrease in buoyant molecular mass for DPGN over the temperature range used in this study. This is already taken into account in the transformation to standard conditions in Figures 5−7 and by the division with the expected temperature-dependent buoyancy factor (eq 8) in Figures 8 and 9. Without this correction, the overall decrease in the buoyant molar mass apparent, for example, from Figures 8 and 9, would be even larger.

Are the movement and associated changes feasible given what we know about plasminogen? There is no crystal structure of the entire protein, but there are structures for all of the kringles and the proteolytic domain. Importantly, there is a structure for kringles 1−3 (*31*). Modeling of this structure with Swiss Protein Data Bank Viewer allows one to apply torsions to the angles around the bonds of Glu63, the first of the three peptide bonds in the linker chain between kringles 1 and 2. One can easily manipulate the relative positions of kringles 1 and 2/3 without incurring any close contacts. We have built a "styrofoam-ball" model of plasminogen (Figure 10); we respected the linker distances between kringles, as well as the covalent bond between kringles 2 and 3. We also respected the linker distance between kringle 5 and the proteolytic domain and the linker distance between Lys50 (the internal ligand to kringle 5) and kringle 1. The styrofoam model indicates that there is sufficient flexibility such that both compact and extended forms of plasminogen are possible. It is interesting to note that the model predicts close contact between kringle 2 and the catalytic domain in the compact form. As the temperature

is lowered, the catalytic domain swings out, and the relative positions of kringles 1 and 2 and the catalytic domain change; kringle 2 and the catalytic domain are no longer adjacent.

We have estimated the thermal midpoint of the transition between the compact (high-temperature) and extended (low-temperature) forms of closed DPGN; it is close to 0 °C (Figure 8A,B). On the basis of estimations of the midpoints and the slopes of Figure 8A,B, we have estimated the thermodynamic parameters for the equilibrium of eq 9. Our bias is to ascribe the changes in hydration/solute binding/voids to hydration. If this is true, the hydration/movement is promoted by an enthalpy term of $10^1$ kcal mol$^{-1}$. Increasing temperature above the midpoint promotes water loss, and this is promoted by the entropy term $-T\Delta S$. Water loss from the protein into the bulk solution results in a large $\Delta S$ (*35*−*37*). As temperature decreases below 15 °C, the product term $s_{20,w}(f/f_0)$ increases, indicating an increase in buoyant molecular mass. As temperature decreases below 15 °C, the product $s_T R6\pi\eta/(1 - \bar{v}_2\rho)$ increases, indicating an increase in buoyant molecular mass. We propose that this apparent increase is the result of the increased hydration of the kringles as they move away from one another; water at the protein surface occupies less space than in the bulk and has a higher density [see Kornblatt and Kornblatt for a relatively recent review (*36*)]. It is worth pointing out that hemoglobin undergoes a similar transition and that it is also promoted by hydration/dehydration (*38*, *39*) with a midpoint transition close to 0 °C (*40*). The transition in the hemoglobin case is T to R. T state Hb is favored by low temperature and hydration; R state Hb is favored by higher temperatures. T state Hb is favored by an enthalpy term of 16.7 kcal mol$^{-1}$ whereas R state is favored by the entropy term (*40*). The structural changes occurring in the T to R transition of Hb are large but do not approach in magnitude the changes seen in the plasminogen system described here. Is it possible to calculate the number of waters associated with the equilibrium between $DPGN^{LT}$ and $DPGN^{HT}$? In principle, the answer is yes, but the data presented here are not yet refined sufficiently, and the uncertainty of the partial specific volumes is too large, as to yield a reliable number. Values in the hundreds of water molecules associated with conformational changes have been reported for other proteins (*38*, *39*, *41*, *42*), and one could speculate that a similar order of magnitude may result in detectable changes in the buoyant molar mass, such as observed in the present study.

## ACKNOWLEDGMENT

We thank the Concordia University Center for Structural and Functional Genomics for the use of their analytical ultracentrifuge and Drs. Peter Ulycznyj and M. J. Kornblatt for helpful discussions.

## REFERENCES

1. Ponting, C. P., Marshall, J. M., and Cederholm-Williams, S. A. (1992) Plasminogen: a structural review, *Blood Coagulation Fibrinolysis 3*, 605−614.
2. Bachmann, F. (1994) Molecular aspects of plasminogen, plasminogen activators and plasmin, in *Haemostasis and Thrombosis* (Bloom, A. L., Forbes, C. D., Thomas, D. P., and Tuddenham, E. G. D., Eds.) pp 525−600, Chuchill Livingston, Edinburgh, U.K.
3. Sottrup-Jensen, L., Zajdel, M., Claeys, H., Petersen, T. E., and Magnusson, S. (1975) Amino-acid sequence of activation cleavage site in plasminogen: homology with "pro" part of prothrombin, *Proc. Natl. Acad. Sci. U.S.A. 72*, 2577−2581.
4. Miles, L. A., Castellino, F. J., and Gong, Y. (2003) Critical role for conversion of glu-plasminogen to lys-plasminogen for optimal stimulation of plasminogen activation on cell surfaces, *Trends Cardiovasc. Med. 13*, 21−30.
5. Ohyama, S., Harada, T., Chikanishi, T., Miura, Y., and Hasumi, K. (2004) Nonlysine-analog plasminogen modulators promote autoproteolytic generation of plasmin(ogen) fragments with angiostatin-like activity, *Eur. J. Biochem. 271*, 809−820.
6. Alkjaersig, N., Fletcher, A. P., and Sherry, S. (1959) vi-Aminocaproic acid: an inhibitor of plasminogen activation, *J. Biol. Chem. 234*, 832−837.
7. Cockell, C. S., Marshall, J. M., Dawson, K. M., Cederholm-Williams, S. A., and Ponting, C. P. (1998) Evidence that the conformation of unliganded human plasminogen is maintained via an intramolecular interaction between the lysine-binding site of kringle 5 and the N-terminal peptide, *Biochem. J. 333* (Part 1), 99−105.
8. Marshall, J. M., Brown, A. J., and Ponting, C. P. (1994) Conformational studies of human plasminogen and plasminogen fragments: evidence for a novel third conformation of plasminogen, *Biochemistry 33*, 3599−3606.
9. Christensen, U. (1984) The AH-site of plasminogen and two C-terminal fragments. A weak lysine-binding site preferring ligands not carrying a free carboxylate function, *Biochem. J. 223*, 413−421.
10. Brockway, W. J., and Castellino, F. J. (1972) Measurement of the binding of antifibrinolytic amino acids to various plasminogens, *Arch. Biochem. Biophys. 151*, 194−199.
11. Castellino, F. J., Brockway, W. J., Thomas, J. K., Liano, H. T., and Rawitch, A. B. (1973) Rotational diffusion analysis of the conformational alterations produced in plasminogen by certain antifibrinolytic amino acids, *Biochemistry 12*, 2787−2791.
12. Tranqui, L., Prandini, M. H., and Suscillon, M. (1979) Structure of fibrinogen and its derivatives: an electron microscope study, *Thromb. Haemostasis 41*, 655−661.
13. Mangel, W. F., Lin, B. H., and Ramakrishnan, V. (1990) Characterization of an extremely large, ligand-induced conformational change in plasminogen, *Science 248*, 69−73.
14. Ponting, C. P., Holland, S. K., Cederholm-Williams, S. A., Marshall, J. M., Brown, A. J., Spraggon, G., and Blake, C. C. (1992) The compact domain conformation of human Glu-plasminogen in solution, *Biochim. Biophys. Acta 1159*, 155−161.
15. Castellino, F. J., and Powell, J. R. (1981) Human plasminogen, *Methods Enzymol. 80* (Part C), 365−378.
16. Kornblatt, J. A., Rajotte, I., and Heitz, F. (2001) Reaction of canine plasminogen with 6-aminohexanoate: a thermodynamic study combining fluorescence, circular dichroism, and isothermal titration calorimetry, *Biochemistry 40*, 3639−3647.
17. Schuck, P. (1998) Sedimentation analysis of noninteracting and self-associating solutes using numerical solutions to the Lamm equation, *Biophys. J. 75*, 1503−1512.
18. Schuck, P., and Demeler, B. (1999) Direct sedimentation analysis of interference optical data in analytical ultracentrifugation, *Biophys. J. 76*, 2288−2296.
19. Schuck, P. (2000) Size-distribution analysis of macromolecules by sedimentation velocity ultracentrifugation and lamm equation modeling, *Biophys. J. 78*, 1606−1619.
20. Schuck, P., Perugini, M. A., Gonzales, N. R., Howlett, G. J., and Schubert, D. (2002) Size-distribution analysis of proteins by analytical ultracentrifugation: strategies and application to model systems, *Biophys. J. 82*, 1096−1111.
21. Dam, J., Velikovsky, C. A., Mariuzza, R. A., Urbanke, C., and Schuck, P. (2005) Sedimentation velocity analysis of heterogeneous protein−protein interactions: Lamm equation modeling and sedimentation coefficient distributions c(s), *Biophys. J. 89*, 619−634.
22. van Holde, K. E. (1975) *Sedimentation Analysis of Proteins*, 4 ed., pp 225−291, Academic Press, New York.
23. Laue, T. M., Shaw, B. D., Ridgeway, T. M., and Pelletier, S. L. (1992) Computer-aided interpretation of analytical sedimentation data for proteins, in *Analytical Ultracentrifugation in Biochemistry and Polymer Science* (Harding, S. E., Rowe, A. J., and Horton, J. C., Eds.) pp 90−125, The Royal Society of Chemistry, Cambridge, U.K.
24. Perkins, S. J. (1986) Protein volumes and hydration effects. The calculations of partial specific volumes, neutron scattering match-

points and 280-nm absorption coefficients for proteins and glycoproteins from amino acid sequences, *Eur. J. Biochem. 157*, 169−180.
25. Cohn, E. J., McMeekin, T. L., Edsall, J. T., and Blanchard, M. H. (1934) Studies in the physical chemistry of amino acids, peptides and related substances. I. The apparent molal volume and the electrostriction of the solvent, *J. Am. Chem. Soc. 56*, 784−794.
26. Durchschlag, H. (1986) Specific volumes of biological macromolecules and some other molecules of biological interest, in *Thermodynamic Data for Biochemistry and Biotechnology* (Hinz, H.-J., Ed.) pp 45−128, Springer, Berlin.
27. Dam, J., and Schuck, P. (2004) Calculating sedimentation coefficient distributions by direct modeling of sedimentation velocity profiles, *Methods Enzymol. 384*, 185−212.
28. Dam, J., and Schuck, P. (2005) Sedimentation velocity analysis of heterogeneous protein−protein interactions: Sedimentation coefficient distributions c(s) and asymptotic boundary profiles from Gilbert-Jenkins theory, *Biophys. J. 89*, 651−666.
29. Christensen, U., and Molgaard, L. (1992) Positive co-operative binding at two weak lysine-binding sites governs the Glu-plasminogen conformational change, *Biochem. J. 285* (Part 2), 419−425.
30. Swindells, J. F., Coe, J. R., Jr., and Godfrey, T. B. (1952) Absolute viscosity of water at 20 °C, *J. Res. Natl. Bur. Stand. 48*, 1−31.
31. Abad, M. C., Arni, R. K., Grella, D. K., Castellino, F. J., Tulinsky, A., and Geiger, J. H. (2002) The X-ray crystallographic structure of the angiogenesis inhibitor angiostatin, *J. Mol. Biol. 318*, 1009−1017.
32. Kornblatt, J. A. (2000) Understanding the fluorescence changes of human plasminogen when it binds the ligand, 6-aminohexanoate: a synthesis, *Biochim. Biophys. Acta 1481*, 1−10.
33. Weisel, J. W., Nagaswami, C., Korsholm, B., Petersen, L. C., and Suenson, E. (1994) Interactions of plasminogen with polymerizing fibrin and its derivatives, monitored with a photoaffinity cross-linker and electron microscopy, *J. Mol. Biol. 235*, 1117−1135.
34. Banyai, L., and Patthy, L. (1985) Proximity of the catalytic region and the kringle 2 domain in the closed conformer of plasminogen, *Biochim. Biophys. Acta 832*, 224−227.
35. Lumry, R., and Rajender, S. (1970) Enthalpy-entropy compensation phenomena in water solutions of proteins and small molecules: a ubiquitous property of water, *Biopolymers 9*, 1125−1227.
36. Kornblatt, J. A., and Kornblatt, M. J. (2002) The effects of osmotic and hydrostatic pressures on macromolecular systems, *Biochim. Biophys. Acta 1595*, 30−47.
37. Kornblatt, J. A., and Kornblatt, M. J. (2002) Water as it applies to the function of enzymes, *Int. Rev. Cytol. 215*, 49−73.
38. Colombo, M. F., Rau, D. C., and Parsegian, V. A. (1992) Protein solvation in allosteric regulation: a water effect on hemoglobin, *Science 256*, 655−659.
39. Colombo, M. F., and Bonilla-Rodriguez, G. O. (1996) The water effect on allosteric regulation of hemoglobin probed in water/glucose and water/glycine solutions, *J. Biol. Chem. 271*, 4895−4899.
40. Imai, K. (1979) Thermodynamic aspects of the co-operativity in four-step oxygenation equilibria of haemoglobin, *J. Mol. Biol. 133*, 233−247.
41. Reid, C., and Rand, R. P. (1997) Probing protein hydration and conformational states in solution, *Biophys. J. 72*, 1022−1030.
42. Rand, R. P. (2004) Probing the role of water in protein conformation and function, *Philos. Trans. R. Soc. London, Ser. B 359*, 1277−1284.
43. Schuck, P., Taraporewala, Z., McPhie, P., and Patton, J. T. (2001) Rotavirus nonstructural protein NSP2 self-assembles into octamers that undergo ligand-induced conformational changes, *J. Biol. Chem. 276*, 9679−9687.

BI050895Y